Journal of Alloys and Compounds 472 (2009) 535–539

Contents lists available at ScienceDirect

Journal of Alloys and Compounds

journal homepage: www.elsevier.com/locate/jallcom

Effect of mechanical activation on structure and thermal decomposition of aluminum sulfate

M. Ghasri-Khouzani, M. Meratian*, M. Panjepour

Department of Materials Engineering, Isfahan University of Technology, 84156-83111 Isfahan, Iran

ARTICLE INFO

Article history:
Received 25 February 2008
Received in revised form 5 May 2008
Accepted 6 May 2008
Available online 7 July 2008

Keywords:
Aluminum sulfate
Mechanical activation
Thermal decomposition
Thermogravimetry

ABSTRACT

The thermal decompositions of both non-activated and mechanically activated aluminum sulfates were studied by thermogravimetry (TG). The structural disorder, the specific surface area (SSA) and the morphology of mechanically activated aluminum sulfates were analyzed by X-ray diffraction (XRD), laser particle-size analyzer, and scanning electron microscopy (SEM), respectively. Thermal analyses results indicated that the initial temperature of thermal decomposition (T_i) in TG curves for mechanically activated aluminum sulfates decreased gradually with increasing the milling time. It was also found that the SSA of mechanically activated aluminum sulfates remained almost constant after a certain milling time, and lattice strains (ε) rose but the crystallite sizes (D) decreased with increasing the milling time. These results showed that the decrease of T_i in TG curves of mechanically activated aluminum sulfates was mainly caused by the increase of lattice distortions and decrease of the crystallite sizes with increasing the milling time.

1. Introduction

Aluminum sulfate ($Al_2(SO_4)_3$), incorrectly called alum, is produced as white crystals which are non-combustible and soluble in water. It is mainly used in paper sizing to improve durability and ink receptivity [1,2], and in water treatment to clarify water [3,4]. Other uses for alum include cellulosic insulation, catalyst, tanning, pharmaceutical preparation, modification of concrete, mordant in dyeing, and manufacture of chemicals [5].

The term "mechanical activation" refers to those processes which are effected by mechanical energy and which involve an increase in the chemical reactivity of the system, but without altering its chemical composition [6]. The process of activation depends on the breakage process and the rate at which energy is supplied to the system. Mechanical treatment of solids by intensive milling has been applied for a variety of reasons including the mechanical alloying of metallic and ceramic powders [7–10], the synthesis of compounds [11–13], phase transformations [9,14], and acceleration of chemical reactions [15–17]. Moreover, it is well known that mechanical activation of solids leads to decreasing decomposition temperature, which is attributed to the increased specific surface area (SSA), enhanced surface reactivity and change in the crystalline structure [18–20].

Thermal decomposition of aluminum sulfate is one possible way of obtaining high-purity, fine-grained aluminum oxide. The chemical reaction involved in the process is thought to be

$$Al_2(SO_4)_3 \rightarrow Al_2O_3 + 3SO_3\uparrow \quad (1)$$

In order to completely convert aluminum sulfate to Al_2O_3 and SO_3, it is necessary to heat at temperatures higher than 1273 K [21]. However, a lower decomposition temperature can be applied by introduction of a reducing agent to the gaseous phase [22]. On the other hand, as it was mentioned before, mechanical treatment of starting materials is one of the latest techniques in this field. To our knowledge, there is no study in the literature dealing with thermal decomposition of mechanically activated aluminum sulfate. This is of special interest, because of the recent application for aluminum sulfate in fabrication of alumina-reinforced aluminum matrix composites [23], where casting temperature is determined by decomposition temperature of aluminum sulfate. So the objective of this research is to investigate the influence of mechanical activation on the thermal decomposition of aluminum sulfate.

2. Experimental

The raw material used in this study was aluminum sulfate octadecahydrate (Merck, Germany), with the following composition (wt.%): $Al_2(SO_4)_3\cdot 18H_2O$, 99.3; chloride, 0.005; ammonium, 0.005; alkali and alkaline earth metals, 0.4; heavy metals, 0.002; Fe, 0.005; Ca, 0.02; K, 0.2 and As, 0.001. The starting material was initially dehydrated at 623 K for 1 h to obtain anhydrous aluminum sulfate and then it was crushed into sub-millimeter-size powder.

---

* Corresponding author. Tel.: +98 3113915722; fax: +98 3113912752.
E-mail address: meratian@cc.iut.ac.ir (M. Meratian).

0925-8388/$ – see front matter © 2008 Elsevier B.V. All rights reserved.
doi:10.1016/j.jallcom.2008.05.012

Mechanical activation of anhydrous aluminum sulfate was performed in a planetary ball mill using hardened chromium steel vials and balls under air atmosphere. Milling was carried out at a rotation rate of 580 rpm with a powder-to-ball mass ratio of 1:15. Mechanically activated aluminum sulfates were obtained after milling for $t_m = 1, 2, 3, 4$ and 5 h.

Thermogravimetry (TG) analyses were carried out on a Linseis L70/2171 instrument with temperature program from 25 to 1020 °C at the heating rate of 10 K min^{-1}, using alumina sample holders with a height of 5 and an internal diameter of 6 mm. The mass of the samples was almost 14 mg. The tests were made under pure argon with flowing rate of 0.33 L min^{-1}.

The structural disorder of all samples was obtained by X-ray diffraction analysis on a Philips X'pert-MPD Diffractometer in the following regime: radiation Cu Kα; $\lambda = 0.15406$ nm; voltage 40 kV; current 30 mA. The degree of amorphization (A) of the samples was determined from X-ray diffraction patterns using following equation [24]:

$$A = \left(1 - \frac{U_0}{I_0} \times \frac{I_x}{U_x}\right) \times 100 \qquad (2)$$

where U_0 and U_x refer to the background of non-activated and mechanically activated samples, while I_0 and I_x are integral intensities of diffraction lines of non-activated and mechanically activated samples.

The Cauchy–Gaussian approximation was used to determine the crystallite size (D) and the equivalent lattice strain (ε) from the XRD data [25]. The morphology of starting material and products was analyzed using a Philips-XL30 Scanning Electron Microscope.

The change of specific surface area with milling time was calculated statistically from the corresponding particle-size distribution data measured on a Fristch A22 Laser Particle-size Analyzer, where ethanol was used as a dispersing fluid.

3. Results and discussion

3.1. TG and DTG results

TG and DTG curves of the decomposition of non-activated and mechanically activated aluminum sulfates are shown in Fig. 1a and b, respectively. Fig. 1a shows that the TG curve for decomposition of non-activated aluminum sulfate exhibits one weight loss that can be identified from change in slope of the curve. In the case of mechanically activated aluminum sulfates, a small weight loss prior to main weight loss is seen in the TG curves (Fig. 1a). This indicates a small part of these samples are mechanically activated more than the rest, and start to decompose at lower temperatures. For all samples, the total weight losses correspond to the theoretical stoichiometry: 70.2 wt.%, i.e. the decomposition process is completed with the formation of Al_2O_3 [21]. The conversions of non-activated and main part of mechanically activated aluminum sulfates to alumina are also observed as minima in the DTG curves (Fig. 1b).

Table 1 shows the influence of milling time on the characteristic temperatures of thermal decomposition in the TG and DTG curves: initial temperature of more activated part (T_i^*) and initial temperature (T_i), peak temperature (T_p), and final temperature (T_f) of main part. The location of these temperatures in TG and DTG curves of 5 h activated aluminum sulfate is shown in Fig. 2. Table 1 reveals that the characteristic temperatures in the TG and DTG curves for different aluminum sulfates decrease gradually with increased milling time. Therefore, as a result of mechanical activation, the reactivity of the solid is enhanced. The results are consistent with observations from thermal studies of ground galenas [20].

Table 1
Influence of milling time on the characteristic temperatures of thermal decomposition of aluminum sulfate

Milling time (h)	T_i^* (K)	T_i (K)	T_p (K)	T_f (K)
0	–	928	1198	1262
1	410	891	1177	1236
2	388	835	1146	1214
3	363	807	1101	1181
4	329	787	1081	1170
5	323	764	1045	1142

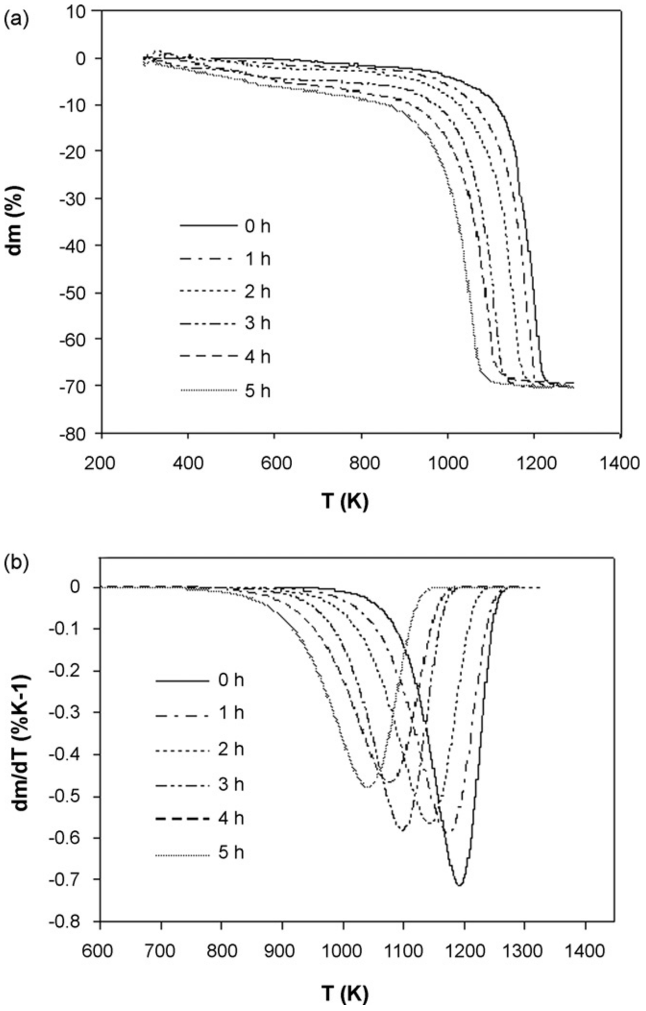

Fig. 1. TG (a) and DTG (b) curves for non-activated and mechanically activated aluminum sulfates.

3.2. X-ray diffraction analysis

The X-ray diffraction patterns for non-activated and mechanically activated aluminum sulfates are shown in Fig. 3. All the peaks can be indexed to aluminum sulfate (JCPDS card no. 30-0043), indicating that aluminum sulfate did not undergo any significant reaction or phase change during milling. It is also seen that the XRD curves of the activated samples are broader and of lower intensity than those of the non-activated sample. This is mainly due to the combined effects of milling such as partial amorphization, structural disordering and defects concentration. By analyzing the (0 1 2), (1 0 4), (1 1 3) and (0 2 4) XRD reflections of non-activated and mechanically activated aluminum sulfates, the degree of amorphization (A), the crystallite sizes (D), and the lattice strains (ε) values are obtained. The variation of the degree of amorphization of aluminum sulfate as a function of milling time is depicted in Fig. 4. Assuming that the non-activated aluminum sulfate was 100% crystalline prior to milling treatment, the calculated degree of amorphization of aluminum sulfate milled for 1 and 5 h were 26% and 53.2%, respectively. The increase of X-ray amorphous phase due to intensive milling was also reported for sulfides [26]. The amorphization is in fact a highly distorted periodicity of lattice elements,

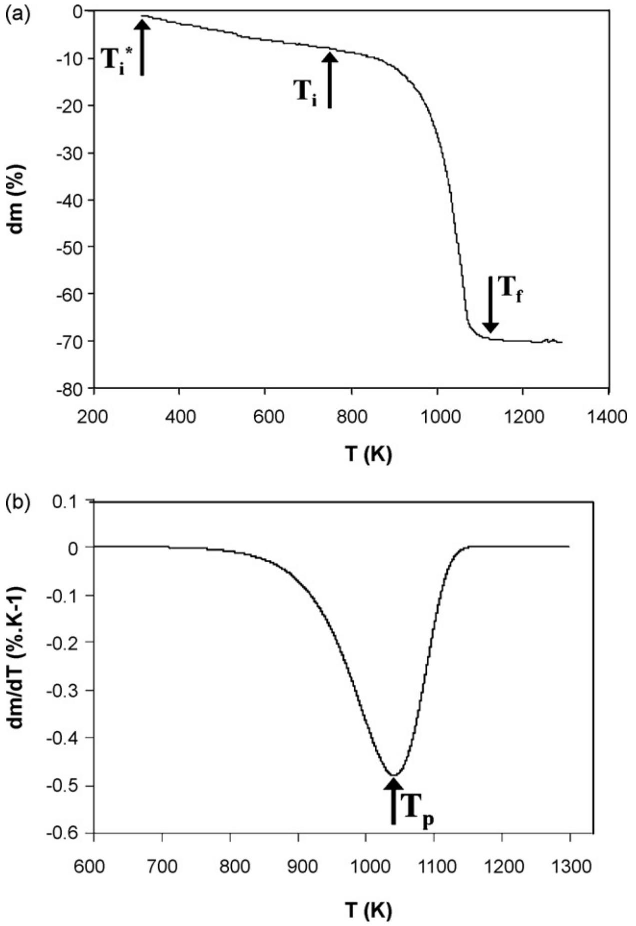

Fig. 2. Location of characteristic temperatures in TG (a) and DTG (b) curves of 5 h activated aluminum sulfate.

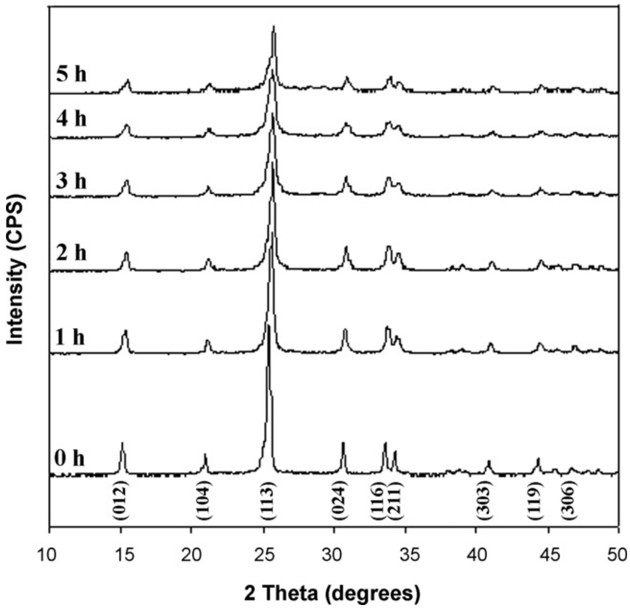

Fig. 3. XRD patterns of non-activated and mechanically activated aluminum sulfates.

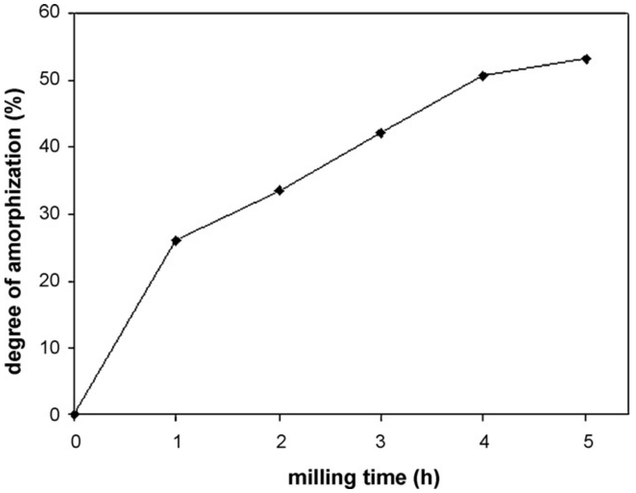

Fig. 4. Change in degree of amorphization for aluminum sulfate with milling time.

and it is often characterized as a short-range order in contrast to the long-range order of a fully crystalline structure.

The change of the crystallite size and lattice strain of aluminum sulfate with milling time is shown in Fig. 5. It is seen that that crystallite sizes decrease strongly up to 3 h milling time, but for superior milling time, reduction rate of crystallite sizes decreases. One can also observe that the values of the lattice strains increase rapidly with milling time up to 3 h and then stabilize for higher milling times.

3.3. SEM observation

Figs. 6 and 7 display the SEM micrographs of the non-activated aluminum sulfate and of the powder obtained after milling for 4 h. The non-activated powder (Fig. 6) consists of angular particles, and their apparent diameter is comprised between 10 and 90 μm. After 4 h of milling, the size and the shape of the particles change dramatically with the apparition of small aggregates (Fig. 7a). Indeed, the milled powders are mainly constituted of coarse particle agglomerates of irregular morphology with a wide size distribution. As revealed by enlarged micrograph of the milled sample (Fig. 7b), these large agglomerates, which can exceed 20 μm in diameter,

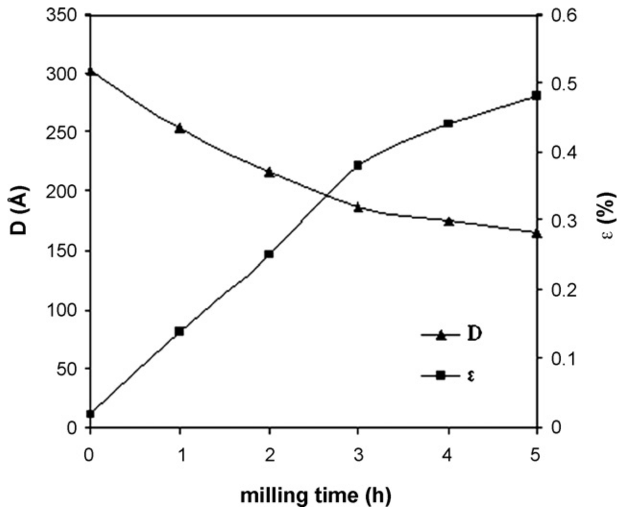

Fig. 5. Dependence of D and ε of mechanically activated aluminum sulfates vs. the milling time.

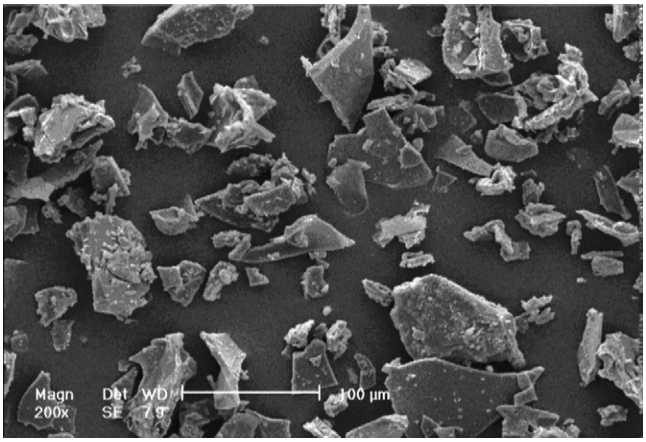

Fig. 6. SEM micrograph of non-activated aluminum sulfate.

are built of fine particles with sizes well inferior to 0.1 µm. The agglomeration of particles during extended dry milling was also reported for titanium dioxide [27]. This behavior is common during dry milling and is usually explained by agglomeration of the structurally modified particles following the initial reduction of particle size. This occurs because of the tendency of the activated material to reduce its surface free energy.

3.4. The specific surface area

The specific surface area of mechanically activated aluminum sulfates versus the milling time is shown in Fig. 8. The specific surface area increases sharply from 0.3 m^2/g for non-activated sample to 6.8 m^2/g for the 3 h activated sample followed by a slight decrease and then stabilizes for higher milling time due to the formation of dense agglomerates. This trend implies that for $t_m < 3$ h, the decrease of T_i in the TG curves of activated aluminum sulfates is caused by increase of the specific surface area as well as the increase of the structural disorder, but for $t_m > 3$ h, the role of specific surface area diminishes.

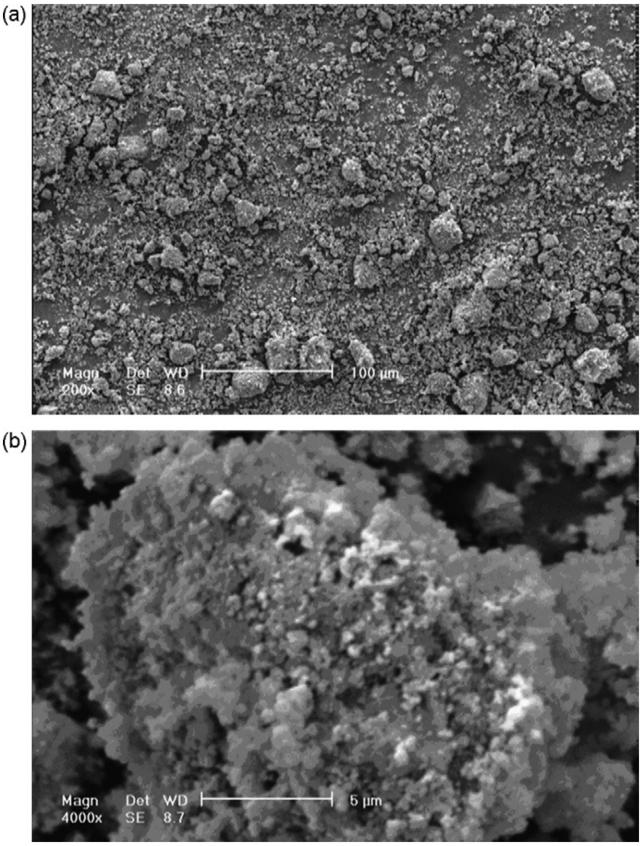

Fig. 7. SEM micrographs of aluminum sulfate mechanically activated for 4 h in two different magnifications.

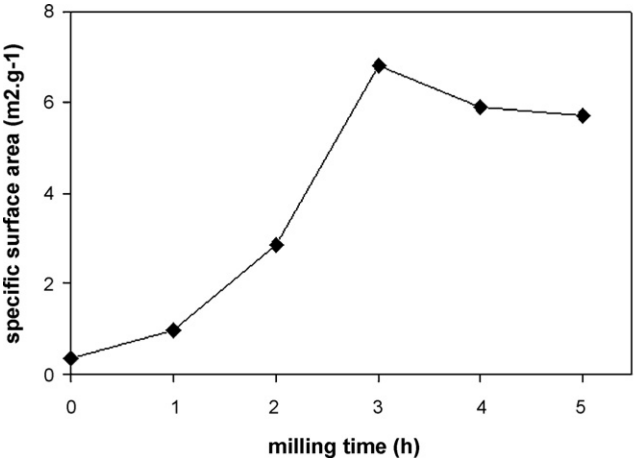

Fig. 8. The specific surface area (SSA) of mechanically activated aluminum sulfates vs. the milling time.

4. Conclusion

Aluminum sulfate does not undergo any reaction or phase change during high-energy ball milling. The initial temperature for thermal decomposition of aluminum sulfates in the TG curves decreases gradually with increased milling time of mechanically activated aluminum sulfates. This mainly arises from the increases of the structural disorder and specific surface area. Mechanically activated aluminum sulfate is more easily subjected to thermal decomposition than non-activated one.

References

[1] B.P. Awate, K.B. Raut, R.K. Khosla, S.C. Shenoy, A. Kumar, S.C. Jhanji, IPPTA 17 (2005) 45.
[2] A.L. Dupont, J. Chromatogr. A 950 (2002) 113.
[3] F. Ciner, A. Eker, Desalination 211 (2007) 102.
[4] W. Lee, P. Westerhoff, Water Res. 40 (2006) 3767.
[5] K. Othmer, Encyclopedia of Chemical Technology, vol. 2, fourth ed., Wiley-Interscience, New York, 1999.
[6] A.Z. Juhasz, L. Opoczky, Mechanical Activation of Minerals by Grinding: Pulverising and Morphology of Particles, Akademia Kiado, Budapest, 1990 (Chapter 1).
[7] J.S. Blázqueza, V. Francoa, C.F. Condea, A. Conde, Intermetallics 15 (2007) 1351.
[8] C. Aguilar, S. Ordonez, J. Marin, F. Castro, V. Martinez, Mater. Sci. Eng. A 464 (2007) 288.
[9] S. Bera, I. Manna, Mater. Sci. Eng. A 417 (2006) 110.
[10] M. Besterci, Mater. Des. 27 (2006) 416.
[11] K. Aoyagi, T. Hiraki, R. Sivakumar, T. Watanabe, T. Akiyama, J. Alloys Compd. 441 (2007) 236.
[12] V. Berbenni, C. Milanese, G. Bruni, A. Marini, Mater. Chem. Phys. 100 (2006) 251.
[13] S. Kumar, A. Bandopadhyay, T.C. Alex, R. Kumar, Ceram. Int. 32 (2006) 555.
[14] P. Xiaoyan, C. Yi, M. Xueming, Z. Lihui, J. Am. Ceram. Soc. 87 (2004) 1164.
[15] E. Rodriguez-Reyna, A.F. Fuentes, M. Maczka, J. Hanuza, K. Boulahya, U. Amador, J. Solid State Chem. 179 (2006) 522.
[16] N.I. Radishevskaya, L.A. Egorova, Y.S. Naiborodenko, N.G. Kasatskii, O.K. Lepakova, Inorg. Mater. 39 (2003) 1288.
[17] F. Kucuk, K. Yildiz, Thermochim. Acta 448 (2006) 107.
[18] H. Hu, Q. Chen, Z. Yin, P. Zhang, Thermochim. Acta 398 (2003) 233.
[19] J. Aquilar-Santillan, R. Cuenca-Alvarez, H. Balmori-Ramirez, R.C. Bradt, J. Am. Ceram. Soc. 85 (2002) 2425.
[20] H. Hu, Q. Chen, Z. Yin, P. Zhang, L. Ye, Metall. Mater. Trans. A 34A (2003) 793.

[21] Y. Pelovski, W. Pietkova, I. Gruncharov, B. Pacewska, J. Pysiak, Thermochim. Acta 205 (1992) 219.

[22] Y. Pelovski, W. Pietkova, I. Gruncharov, B. Pacewska, J. Pysiak, Thermochim. Acta 205 (1992) 238.

[23] O. Liuzhang, L. Chengping, S. Xiandong, Z. Meiqin, Z. Min, Mater. Lett. 57 (2003) 1712.

[24] S.M. Ohlberg, D.W. Strickler, J. Am. Ceram. Soc. 45 (1962) 170.

[25] H.P. Klug, L. Alexander, X-ray Diffraction Procedures for Polycrystalline and Amorphous Materials, second ed., Wiley-Interscience, New York, 1974 (Chapter 9).

[26] K. Tkacova, Mechanical Activation of Minerals, Elsevier, Amsterdam, 1989.

[27] R. Ren, Z. Yang, L.L. Shaw, J. Mater. Sci. 35 (2000) 6015.